AMERICAN JOURNAL OF PHYSICAL ANTHROPOLOGY 90:207–213 (1993)

Radiographic Estimation of Long Bone Cross-Sectional Geometric Properties

JACQUELINE A. RUNESTAD, CHRISTOPHER B. RUFF, JAMES C. NIEH, RICHARD W. THORINGTON, JR. AND MARK F. TEAFORD
Department of Cell Biology and Anatomy, Johns Hopkins University School of Medicine, Baltimore, Maryland 21205 (J.A.R., C.B.R., M.F.T.) and Division of Mammals, National Museum of Natural History, Smithsonian Institution, Washington, DC 20560 (J.C.N., R.W.T.)

KEY WORDS Biomechanics, Small mammals, Diaphyses, Imaging techniques

ABSTRACT Because of their biomechanical significance, cross-sectional geometric properties of long bone diaphyses (areas, second moments of area) have been increasingly used in a number of form/function studies, e.g., to reconstruct body mass or locomotor mode in fossil primates or to elucidate allometric scaling relationships among extant taxa. In the present study, we test whether these biomechanical section properties can be adequately estimated using biplanar radiographs, as compared to calculations of the same properties from computer digitization of cross-sectional images. We are particularly interested in smaller animals, since the limb bone cortices of these animals may not be resolvable using other alternative noninvasive techniques (computed tomography). The test sample includes limb bones of small (25–5,000 g) relatively generalized quadrupedal mammals—mice, six species of squirrels, and *Macaca fascicularis*. Results indicate that biplanar radiographs are reasonable substitutes for digitized cross-sectional images for deriving areas and second moments of area of midshaft femora and humeri of mammals in this size range. Potential application to a variety of questions relating to mechanical loading patterns in such animals is diverse.

Patterns of limb mechanical loading should reflect positional behavior and body mass and, hence, have been the focus of many biomechanical studies. Since long bone diaphyses can be modelled as engineering beams (e.g., Huiskes, 1982), cross-sectional diaphyseal properties employed in beam analyses—areas and second moments of area—can be used to draw inferences regarding the mechanical loadings of limbs (Burr et al., 1981, 1982, 1989; Demes and Jungers, 1989; Lovejoy et al., 1976; Ruff, 1987; Ruff and Hayes, 1983a,b; Schaffler et al., 1985). Ideally, cross-sectional properties are calculated through computer digitization of cross-sectional images from natural breaks, sectioned bones, or computerized tomographic (CT) images. However, it is often desirable to substitute radiographs for actual cross-sectional images because: (1) there may be no convenient natural breaks and museum specimens may not be sectioned, (2) CT may not be available and may not produce sufficient resolution below a certain size limit,[1] and (3) X-ray machines are readily available at many institutions, including museums. Measurements of bone

Received December 2, 1991; accepted July 16, 1992.

Address reprint requests to Jacqueline A. Runestad, Dept. of Cell Biology and Anatomy, John Hopkins University School of Medicine, 725 N. Wolfe St., Baltimore, MD 21205.

[1]We have found that long bone cortices less than roughly 1 mm thick are not well resolved by most CT scanners. The majority of the specimens included in this study (all of the mice and squirrels, see below) had cortical thicknesses in this size range.

cortices from radiographs taken in mediolateral and anteroposterior orientations can be used to calculate section properties by using a simplified geometrical model—a circular or elliptical ring—and standard engineering formulae (e.g., Shigley, 1976). Such an approach has been used in a variety of studies, including studies of living people and human cadavers (Klenerman et al., 1967; Smith and Walker, 1964), human archeological and paleontological studies (Ben-Itzhak et al., 1988; Fresia et al., 1990), and studies of extant nonhuman primates (Demes and Jungers, 1989; Demes et al., 1991).

Use of radiographs to estimate digitized section properties involves some extrapolation and assumptions regarding bone cross-sectional shape; however, the validity of such assumptions has been tested only for samples of human humeri (Fresia et al., 1990; Klenerman et al., 1967) and carnivore mandibles (Biknevicius and Ruff, 1992). The purpose of the present study is to compare biomechanical cross-sectional properties calculated from biplanar radiographs to those calculated by computer digitization of cross-sectional images of femora and humeri in smaller mammalian species in order to assess the utility of X-ray data in interpreting loading patterns in the long bones of small mammals. In addition, we address the question of whether a model taking into account differing cortical thicknesses in opposite walls of long bones is more accurate than the more commonly used symmetrical hollow beam model. Biknevicius and Ruff (1992) found that an asymmetrical model better represented carnivore mandibular cross sections.

MATERIALS AND METHODS

Radiographs of associated femora and humeri of four lab mice averaging 25 g (*Mus musculus poschiavinus* bred to *M. m. domesticus*) and of two individuals for each of six sciurid species (*Eutamias minimus, Glaucomys volans, Tamias striatus, Spermophilus lateralis, Sciurus carolinensis,* and *Spermophilus beecheyi*), ranging between 41 and 729 g, from the Smithsonian Institution collections, were X-rayed in standard anterioposterior and mediolateral views (Table 1). (Note that the body mass of an individual squirrel can vary considerably due to seasonal changes in fat storage. Therefore, subspeciesmeans rather than individually associated weights are listed in Table 1.) The dimensions measured in this study were thicknesses of medial, lateral, anterior, and posterior cortices, as well external diameters in both planes. These distances were measured from X-ray images to a nominal precision of 0.001 mm using a Reflex Microscope (Reflex Measurement, Ltd.). This microscope records the position of a central laser point in a set of Cartesian coordinates coupled to the movement of the stage. The X-ray images were positioned on a light box on the stage so that the transverse section to be measured was parallel to the transverse axis of the microscope. As the section was moved under the microscope (via stage movement) along the transverse axis, coordinate positions of the laser point were recorded at periosteal and endosteal boundaries. In this manner, periosteal and endosteal diameters, as well as cortical thicknesses, were measured. To calibrate the microscope, measurements of a glass stage micrometer were repeated eight times, showing a coefficient of variation of only 4% for a breadth of 0.05 mm. To test the precision of the measuring process itself, radiographs of two epoxy resin bone-simulating phantoms (see Ruff and Leo, 1986, fn 9, p. 190) constructed to be in the size range of bones of the larger squirrels (outer diameters 5.3 and 3.5 mm and inner diameters 2.9 and 2.4 mm, respectively), were measured six times. These yielded CVs of less than 1% for repeated measurements of outer and inner diameters of both cylinders. For the actual bone radiographic images used in the

TABLE 1. Specimens and body masses[1]

Specimens	N	Body Mass (g)
lab mice	4	25
Eutamias minimus	2	41
Glaucomys volans	2	77
Tamias striatus	2	107
Spermophilus lateralis	2	180
Sciurus carolinensis	2	550
Spermophilus beecheyi	2	729
Macaca fascicularis, females	5	3240
Macaca fascicularis, males	3	4967

[1] Mouse and macaque body masses are averages of individual weights. Sciurid masses are respective subspecies means of USNM collection.

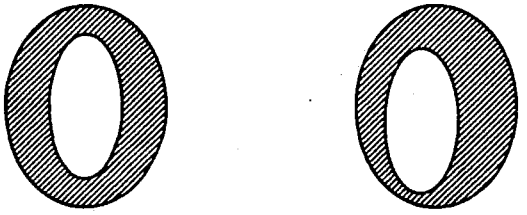

a. symmetrical b. asymmetrical

Fig. 1. Diagrams of symmetrical and asymmetrical cross sections.

analysis, the average CV for >200 individual breadths measured three times each was 2.4%.

The lab mice and squirrel femora and humeri were sectioned at or near midshaft and camera lucida images drawn of the resultant cross sections (magnification 10–25 times). Using a modified version of the computer program SLICE (Nagurka and Hayes, 1980), the images were manually digitized and the geometric properties of the sections calculated (see Ruff and Hayes, 1983a). The results were then compared to calculations based on radiographic measurements taken with the Reflex Microscope.

Radiographic and CT images of femora for five *Macaca fascicularis* females (average weight 3,240 g) and three *M. fascicularis* males (4,967 g) were included from a previous study (Ruff, 1987). Due to their larger size, radiographic images of these specimens were manually measured to 0.1 mm, using needle-nose calipers.

Using a symmetrical hollow beam model, outer (periosteal) and inner (endosteal or medullary) diameters were entered into standard engineering formulae for cortical area and second moments of area (e.g., Shigley, 1976). This model assumes that opposite cortical walls are of equal thickness as shown diagrammatically in Figure 1a (e.g., anterior and posterior walls are the same). Cortical area, CA (a measure of bone axial strength), is calculated as:

$$CA = \pi \times ((\text{ML outer diameter} \times \text{AP outer diameter}) - (\text{ML inner diameter} \times \text{AP inner diameter}))/4$$

AP stands for anteroposterior and ML for mediolateral.

The second moment of area about the coronal plane (Ix) and that about the sagittal plane (Iy) are calculated as:

$$Ix = \pi \times ((\text{ML outer diameter} \times \text{AP outer diameter}^3) - (\text{ML inner diameter} \times \text{AP inner diameter}^3))/64$$

$$Iy = \pi \times ((\text{AP outer diameter} \times \text{ML outer diameter}^3) - (\text{AP inner diameter} \times \text{ML inner diameter}^3))/64$$

The polar second moment of area (J) is simply Ix plus Iy. The term Ix is a measure of bending rigidity in the sagittal plane about a frontal axis, Iy is a measure of bending rigidity in the frontal plane about a sagittal axis, and J corresponds to torsional rigidity (Ruff and Hayes, 1983a).

We also entered the radiographic measurements into formulae for an asymmetrical model that does not assume that opposite cortices are of equal thickness (see Fig. 1b). (These formulae require considerable explanation and are thoroughly discussed in Biknevicius and Ruff, 1992, and are not listed here.) In addition, dummy cortical thicknesses were entered into the formulae, creating one sample with opposite cortical walls of equal thickness and another sample with walls up to twice as thick as opposite walls, keeping inner and outer diameters (and thus cortical areas) the same. This was done to test how dissimilar opposite walls can be before use of the more involved asymmetrical model provides any advantage.

To test the strength of the relationship between digitized and estimated properties, calculations from biplanar radiographs were compared to those from SLICE using the least-squares regression technique (SYSTAT: Wilkinson, 1989).[2] Symmetrical model results were compared to asymmetrical model results using this technique as well. Coefficients of determination (r^2's) and per-

[2]Use of a statistical model accounting for error in both axes, such as Model II (RMA), produces identical results due to very high correlations (see below).

Table 2. Regression statistics of radiograph data vs. digitized cross-sectional data (as derived from SLICE program)[1]

Comparison	r^2	% SEE	Intercept (std. err.)	Slope (std. err.)
Humerus without macaques (N = 16):				
J	0.995	16	−0.064 (0.037)	0.999 (0.019)
IX	0.993	20	−0.015 (0.048)	0.995 (0.023)
IY	0.994	17	−0.115 (0.042)	1.002 (0.020)
CA	0.991	10	−0.025 (0.027)	0.998 (0.025)
Femur with macaques (N = 24):				
J	0.998	16	−0.083 (0.040)	1.030 (0.011)
IX	0.994	28	−0.081 (0.058)	1.029 (0.017)
IY	0.998	15	−0.051 (0.034)	1.029 (0.010)
CA	0.995	12	−0.069 (0.034)[F]	1.043 (0.015)
Femur without macaques (N = 16):				
J	0.992	18	−0.085 (0.043)	1.032 (0.025)
IX	0.975	33	−0.100 (0.072)	1.005 (0.043)
IY	0.994	16	−0.045 (0.037)	1.043 (0.022)
CA	0.985	12	−0.065 (0.035)	1.029 (0.034)

[1] J = polar second moment of area; IX = second moment of area about coronal axis; IY = second moment of area about sagittal axis; CA = cortical area.

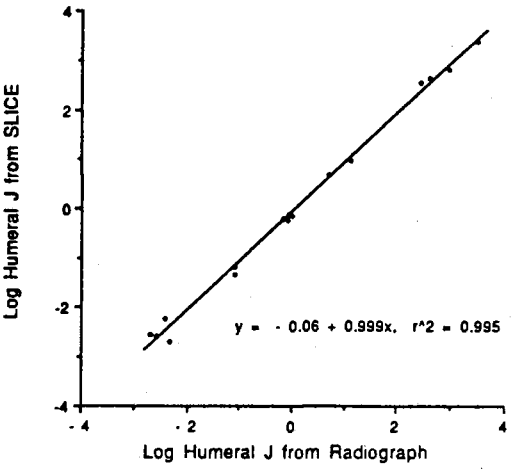

Fig. 2. Humeral midshaft polar second moment of area (J) from radiograph vs. from SLICE in lab mice and squirrels.

cent standard errors of estimate (%SEE's)[3] were used to evaluate the accuracy with which radiographic estimates predicted digitized values. In addition, regression slopes close to one and intercepts close to zero were taken to indicate random rather than directional (e.g., size-related) errors in estimation. Data were log-transformed because of the large size range involved (two orders of magnitude), i.e., to more equally weight smaller and larger specimens in the comparisons. Femoral regressions were run with and without the macaques due to the different techniques employed in obtaining digitized cross-sectional data (rodent data came from camera lucida drawings, macaque data from CT images).

RESULTS

Regression statistics of radiographic data versus corresponding SLICE data (logged) are shown in Table 2. The r^2's are almost all 0.99 or better, with intercepts close to zero and slopes close to one. The %SEE's range between 10% and 20%, except for Ix of the femur (28% with macaques, 33% without macaques). Judging from both the slope and intercept data, the errors in estimation of digitized (SLICE) properties are random rather than directional. Figure 2 illustrates the regression of humeral J values calculated from radiographs on corresponding values from SLICE digitization. As shown in Table 2, none of the regression slopes for the humerus significantly differs from one, and only one of the intercepts for the humerus significantly differs from zero (by analysis of covariance; Zar, 1984). Figure 3 illustrates regression of femoral J values calculated from radiographs on corresponding values from SLICE digitization. Several of the regression slopes and intercepts of the femur shown in Table 2 depart significantly from one or zero, respectively, but all slopes are within 0.05 of one, and all intercepts are within 0.1 of zero.

*Non*logged radiographic data were also considered and yielded results similar to the log-log analyses with r^2's of 0.99 or better, and %SEE's between 10% and 17% for cortical area and polar second moment of area. We consider the log-log results more relevant, however, because the nonlogged anal-

[3] Standard error of the estimate shows the overall accuracy with which a regression-derived formula predicts the value of Y from the value of X (Zar, 1984). The standard error is proportional to the magnitude of Y, the dependent variable. Division by the mean value of Y yields a unitless value, which multiplied by 100 gives %SEE. For logged data, as in most of this analysis, the log SEE is converted to a %SEE following a procedure described by Smith (1984).

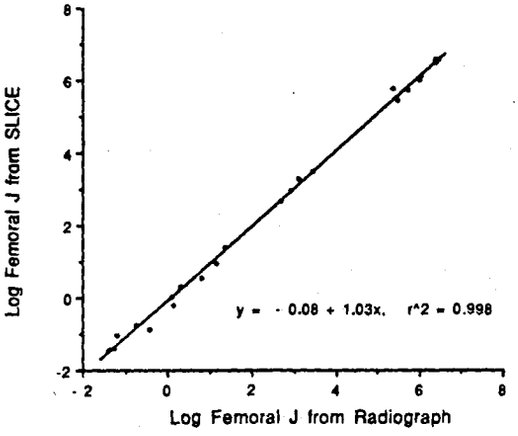

Fig. 3. Femoral midshaft polar second moment of area (J) from radiograph vs. from SLICE in lab mice, squirrels, and macaques.

TABLE 3. Symmetrical hollow beam model vs. asymmetrical hollow beam model statistics[1]

Comparison	r^2	% SEE	Intercept (std. err.)	Slope (std. err.)
Humerus (N = 16):				
J	1.000	0.005	−0.004 (0.001)	1.000 (0.001)
IX	1.000	0.012	−0.008 (0.003)	0.998 (0.001)
IY	1.000	0.005	−0.003 (0.001)	1.001 (0.001)
Femur (N = 24):				
J	1.000	0.004	−0.004 (0.001)	1.000 (0.000)
IX	1.000	0.005	−0.006 (0.001)	1.000 (0.000)
IY	1.000	0.007	−0.002 (0.002)	0.999 (0.001)

[1] For abbreviations see Table 2; femoral data include macaques.

yses tended to be driven by the data scatter of only the larger species.

Results of the symmetrical/asymmetrical hollow beam model comparisons are shown in Table 3 (logged data). All r^2's are one, and none of the slopes are significantly different from one. Statistically, most of the intercepts (−0.008–−0.002) are different from zero, but the standard errors are so small (0.001–0.003) that these differences are taken to be biologically insignificant.

The tests with dummy cortical thicknesses indicated that even asymmetry as great as two to one in thickness of opposite walls (greater than any asymmetry actually present in our bone specimens) had little effect on calculation of second moments of area – r^2's were extremely close to one, slopes were within 0.1 of one, and intercepts were within 0.1 of zero.

DISCUSSION

Our results show that biplanar radiographs are reasonable substitutes for actual cross-sectional images in calculating the section properties (areas and second moments of area) of long bone midshafts in small to medium-size mammals. This is consistent with the high correlations seen in the other two studies which have compared radiographically derived properties to those from digitized cross sections. For example, Fresia et al. (1990) found an r^2 of 0.94 between digitized and estimated polar second moments of area of human humeri (mid-distal location), and Biknevicius and Ruff (1992) found mean percentage deviations of less than 10% for digitized and estimated second moments of area in mandibular sections (asymmetric model).

Results also indicate that the distribution of cortical bone, within single planes, is sufficiently symmetrical in the midregion of humeral and femoral diaphyses to warrant use of the simple hollow beam symmetrical formulae for calculation of cross-sectional geometric properties. This is perhaps not surprising as the regions of the bones sampled were, in fact, chosen because they are relatively regular, i.e., round or oval-shape. However, this is not necessarily true for other regions of the same bones (e.g., the proximal humerus) or other bones (e.g., the tibia), which are less symmetrical and/or regular in contour (Ruff, unpublished data). Biknevicius and Ruff (1992) found that the asymmetrical model better suited mandibular cross sections in carnivores that are strongly asymmetrical in cortical bone distribution. It also may not be valid to generalize our results to other species with very prominent muscle crests, which would cause midshaft cross sections to depart notably from symmetrical elliptical shapes. An example of this would be the highly modified humeri of Oligocene palaeanodonts (probably fossorial), which bear exaggerated muscle crests extending throughout the diaphyses (Rose and Emry, 1983). It is also important to note that maximum and mini-

mum second moments of area and their orientation can only be calculated from actual cross sections. However, for many applications areas and second moments of area about anterior-posterior and medial-lateral axes are sufficient. In addition, as J equals the sum of Ix and Iy, torsional rigidity can be calculated from biplanar images.

Other than basic measurement error and that inherent from relying on biplanar radiographs for calculation of cross-sectional properties, potential error sources here included the control (digitized) estimates themselves. The camera lucida images were made from cut surfaces, some of which were slightly crushed. The process of drawing the images is a less than perfect means of reproducing sections. Digitization of the images is also subject to error. In addition, CT scan resolution decreases with bones as small as macaque femora. Given these other error sources, the data scatter between digitized and estimated properties is remarkably small (Figs. 2, 3).

As radiography is nondestructive and generally accessible, the use of biplanar radiographs to estimate biomechanical cross-sectional properties in long bone diaphyses has considerable potential for diverse applications. The technique is applicable to both extant and fossil specimens, and is limited to neither larger specimens nor those with natural breaks.

ACKNOWLEDGMENTS

The authors thank Linda Coley of the Smithsonian Institution for technical assistance, Dr. Hannah Grausz of Johns Hopkins University for providing lab mice, Dr. Ken Rose of Johns Hopkins University for loan of micrometer and dissecting microscope, the Smithsonian Institution Department of Mammals for access to collections, the Smithsonian Institution Department of Ichthyology for radiographic facilities, the Scholarly Studies Program of the Smithsonian Institution, the Summer Intern Program of the Smithsonian Institution, and the Johns Hopkins University Department of Cell Biology and Anatomy for funds made available to J.A.R. for supplies and travel related to the project.

LITERATURE CITED

Ben-Itzhak S, Smith P, and Bloom RA (1988) Radiographic study of the humerus in Neandertals and *Homo sapiens sapiens*. Am. J. Phys. Anthropol. *77*:231–242.

Biknevicius AR, and Ruff CB (1992) Use of biplanar radiographs for estimating cross-sectional geometric properties of the mandible. Anat. Rec. *232*:157–163.

Burr DB, Piotrowski G, and Miller GJ (1981) Structural strength of the macaque femur. Am. J. Phys. Anthropol. *54*:305–319.

Burr DB, Ruff CB, and Johnson C (1989) Structural adaptations of the femur and humerus to arboreal and terrestrial environments in three species of macaques. Am. J. Phys. Anthropol. *79*:357–367.

Burr DB, Piotrowski G, Martin RB, and Cook PN (1982) Femoral mechanics in the lesser bushbaby (*Galago senegalensis*): Structural adaptations to leaping in primates. Anat. Rec. *202*:419–429.

Demes B, and Jungers WL (1989) Functional differentiation of long bones in lorises. Folia Primatol. *52*:58–69.

Demes B, Jungers WL, and Selpien K (1991) Body size, locomotion and long bone cross-sectional geometry in indriid primates. Am. J. Phys. Anthropol. *86*:537–547.

Fresia AE, Ruff CB, and Larsen CS (1990) Temporal decline in bilateral asymmetry of the upper limb on the Georgia Coast. In CS Larson (ed.): The Archaeology of Mission Santa Catalina de Guale: 2. Biocultural Interpretations of a Population in Transition: Anthropological Papers of the American Museum of Natural History, pp. 121–150.

Huiskes R (1982) On the modelling of long bones in structural analyses. J. Biomech. *15*:65–69.

Klenerman L, Swanson SAV, and Freeman MAR (1967) A method for the clinical estimation of the strength of a bone. Proc. R. Soc. Med. *67*:850–854.

Lovejoy CO, Burstein AH, and Heiple KG (1976) The biomechanical analysis of bone strength: A method and its application to platycnemia. Am. J. Phys. Anthropol. *44*:489–506.

Nagurka ML, and Hayes WC (1980) An interactive graphics package for calculating cross-sectional properties of complex shapes. J. Biomech. *13*:59–64.

Rose KD, and Emry RJ (1983) Extraordinary fossorial adaptations in the Oligocene palaeanodonts *Epoicotherium* and *Xenocranium* (mammalia). J. Morph. *175*:33–56.

Ruff CB (1987) Structural allometry of the femur and tibia in hominoidea and *Macaca*. Folia Primatol., *48*:9–49.

Ruff CB, and Hayes WC (1983a) Cross-sectional geometry of Pecos Pueblo femora and tibiae—a biomechanical investigation: I. Method and general patterns of variation. Am. J. Phys. Anthropol. *60*:359–381.

Ruff CB, and Hayes WC (1983b) Cross-sectional geometry of Pecos Pueblo femora and tibiae—a biomechanical investigation: II. Sex, age, and side differences. Am. J. Phys. Anthropol. *60*:383–400.

Ruff CB, and Leo FP (1986) Use of computed tomography in skeletal structure research. Amer. J. Phys. Anthropol. *29*:181–196.

Schaffler MB, Burr DB, Jungers WL, and Ruff CB (1985) Structural and mechanical indicators of limb specialization in primates. Folia Primatol. *45:*61–75.

Shigley JE (1976) Applied Mechanics of Materials. New York: McGraw-Hill.

Smith RJ (1984) Allometric scaling in comparative biology: Problems of concept and method. Am. J. Physiol. *256:*152–160.

Smith RW, and Walker RR (1964) Femoral expansion in aging women: implications for osteoporosis and fractures. Science *145:*156–157.

Wilkinson L (1989) SYSTAT: The System for Statistics. Evanston, IL.: SYSTAT.

Zar JH (1984) Biostatistical Analysis, 2nd Ed. Englewood Cliffs, NJ.: Prentice-Hall.